PHYSICAL REVIEW A VOLUME 52, NUMBER 2 AUGUST 1995

Influence of spontaneous emission on trapping states and start-up times of degenerate two-photon micromasers

E. S. Guerra, S. M. Dutra, and P. L. Knight
Optics Section, The Blackett Laboratory, Imperial College, London SW7 2BZ, England

N. Zagury
Instituto de Física, Universidade Federal do Rio de Janeiro, Rio de Janeiro, 21945-970, RJ, Brazil
(Received 30 November 1994; revised manuscript received 9 March 1995)

We study degenerate two-photon micromasers pumped by cascade three-level atoms, where each atomic energy level has a different linewidth. Our model allows us to recover the ordinary two-photon micromaser situation when these widths vanish. In the limit of large linewidths we obtain a two-photon laser model. We show that trapping states are extremely sensitive to atomic decay, even when the decay time is small in comparison to the transit time through the cavity. Unlike the one-photon micromaser, they are sensitive to the linewidth of the upper as well as the lower energy level. We have also studied the effects of atomic decay on the starting time of micromasers and on the noise. We found that there is a significant difference between the behavior of two-photon micromasers and lasers as we change the ratio of the widths of the upper and lower levels.

PACS number(s): 42.50.Dv, 42.52.+x

I. INTRODUCTION

Rydberg atoms have very large spontaneous-emission decay times in free space: of the order of $10^{-9}n^3$ s for atomic transitions from a state with principal quantum number n and low orbital angular momentum $l \sim 1$ and of the order of $10^{-9}n^5$ s for transitions from circular states [1]. These are much larger than cavity transit times in micromaser experiments [2,3], which are usually of the order of 10 μs. So, in micromaser theory, atomic decay is normally neglected [4]. However, even such small atomic decay rates can be important in the description of the dynamics of micromasers [5,6].

For one-photon micromasers, it has already been shown that trapping states [7] are very sensitive to atomic decay [5]. Trapping states are highly nonclassical states of the field where there is no more than a given number of photons in the cavity mode. They are the stationary solutions of the micromaser master equation in the limit of zero cavity loss and infinite atomic lifetime. They play a very important role in the dynamics of the one- and two-photon micromasers and have a dramatic effect on the starting time [8]. For values of the pumping parameter corresponding to trapping states for $N = 0$, the two-photon micromaser does not start even if the cavity loss is not negligible, as long as we keep the cavity at zero temperature. This effect is usually eliminated completely by a small velocity distribution in the atomic beam or a low-temperature thermal field. However, there is a certain value of the pumping parameter, for which each atom undergoes an integer number of complete Rabi oscillations, that turns all number states into trapping states of the two-photon micromaser. For this value of the pumping parameter the micromaser never starts, even at nonzero temperature, and the effect persists up to a velocity spread of three percent [8], which would make it possible to be observed in the laboratory. If a small amount of atomic decay can destroy these trapping states, the micromaser will start after all.

We have studied the influence of atomic decay on several properties of two-photon micromasers and show how the role of atomic decay changes when we go from a model of a micromaser to a laser or maser. In Sec. II, we present our model. In Sec. III, we discuss the results of a Fokker-Planck analysis of the transition between the two-photon micromaser and laser model. Then, in Sec. IV, we show that trapping states are extremely sensitive to atomic decay, even when the decay time is small in comparison to the transit time through the cavity and that, unlike the situation in the one-photon micromaser, trapping states are sensitive to the linewidth of the upper, as well as the lower energy level. In Sec. V we discuss how the atomic decay affects the starting time of two-photon micromasers and show that there is a significant difference between the micromaser and the laser regimes. In a laser, decreasing the decay rate of the upper level leads to a decrease in the starting time, while decreasing the decay rate of the lower level will increase it. In a micromaser the smaller the decay rate of the lower level, the shorter the starting time, the upper energy level having very little effect. In Sec. VI we show that reabsorption of photons plays different roles in micromasers and lasers and is an essential part of the noise reduction mechanism in micromasers. Contrary to the well-known result for lasers, the inhibition of reabsorption in micromasers increases the noise. This corroborates the idea that noise reduction in micromasers is mainly a consequence of the coherent exchange of energy between the atom and the cavity mode, which can exist only when reabsorption of photons is allowed. Finally, we summarize our results in Sec. VII.

II. MODEL

We adopt the usual theoretical model for two-photon micromasers [4] with the exception that each energy level of our cascade three-level atoms is allowed to decay to a corresponding lower lying level (see Fig. 1). In this section we describe how we have modified the usual approach to accommodate this.

In our model, cascade three-level atoms are initially prepared in the excited state and injected, one at a time, into a cavity tuned to a frequency ω. $|a\rangle$ and $|c\rangle$ are the upper and lower atomic energy eigenstates and $|b\rangle$ is a relay intermediate state with energy $\hbar\omega_b$ nearly halfway between the atomic energy levels $\hbar\omega_a$ and $\hbar\omega_c$. $\Delta_1 = \omega_a - \omega_b - \omega$ and $\Delta_2 = \omega_b - \omega_c - \omega$ are the detunings between the two one-photon atomic transitions and the cavity frequency. One-photon transitions between $|a\rangle$ and $|c\rangle$ are forbidden. The two-photon micromaser operates on the degenerate two-photon transition $|a\rangle \rightarrow |c\rangle$. We will also assume two-photon resonance $\Delta_1 = -\Delta_2$.

Levels $|a\rangle$, $|b\rangle$, and $|c\rangle$ are considered to be Rydberg levels as in the two-photon micromaser experiment performed by Brune *et al.* [3] Rydberg states can be metastable, but they do eventually decay to lower states. In order to take this into account, we introduce the lower lying states $|a'\rangle$, $|b'\rangle$, and $|c'\rangle$. The idea is that atoms can now make transitions between unprimed states and their primed counterparts. Energy is then transferred from the atom to one of the modes of the reservoir by creating a photon in that mode. Because transitions between unprimed atomic states and primed atomic states involve coupling to a dense set of modes, not to the resonant cavity mode, they are Markovian processes. This yields the typical spontaneous-emission exponential decay of the populations of the unprimed atomic states, which makes these energy levels have a finite linewidth.

We assume that cavity field decay can be treated independently of the interaction of the atoms and the field [4,9–11]. This assumption has been discussed in Ref. [11] and is quite reasonable for micromasers where the mean lifetime of the cavity field is typically of the order of 10^{-2} s for superconducting microwave cavities, while the time each atom spends in the cavity is of the order of 10^{-5} s [2,3].

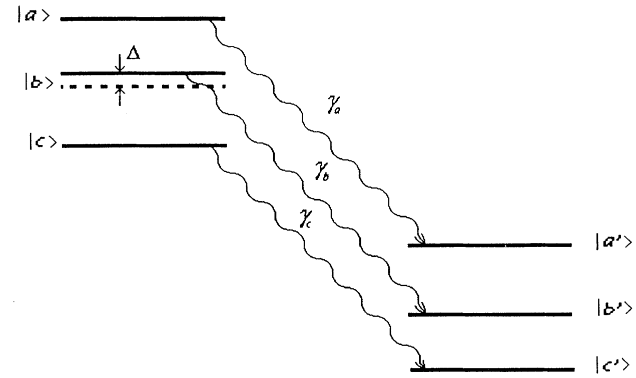

FIG. 1. Energy levels relevant to the two-photon micromaser with atomic decay channels to lower states at rates γ_a, γ_b, and γ_c indicated.

We will now describe the field evolution when there is one atom in the cavity and cavity damping is negligible. Later we will examine how the field evolves in the time interval between two successive atoms, adding the interaction of resonant cavity mode with its reservoir. The Hamiltonian that describes the dynamics of the system in the rotating wave approximation is given by

$$H = \hbar\omega A^\dagger A + \hbar\omega_a|a\rangle\langle a| + \hbar\omega_b|b\rangle\langle b| + \hbar\omega_c|c\rangle\langle c| + \hbar\Omega_{ab}(A|a\rangle\langle b| + A^\dagger|b\rangle\langle a|) + \hbar\Omega_{bc}(A|b\rangle\langle c| + A^\dagger|c\rangle\langle b|) + R \,, \tag{2.1}$$

where Ω_{ab} (Ω_{bc}) are the one-photon Rabi frequencies associated with Rabi oscillations between the levels a and b (b and c), the operator A ($A^\dagger$) is the annihilation (creation) operator for the electromagnetic field mode of frequency ω, and

$$R = \hbar\sum_k \omega_k B_k^\dagger B_k + \hbar\omega_{a'}|a'\rangle\langle a'| + \hbar\omega_{b'}|b'\rangle\langle b'| + \hbar\omega_{c'}|c'\rangle\langle c'| + \hbar\sum_k \Omega_{aa'k}(B_k|a\rangle\langle a'| + B_k^\dagger|a'\rangle\langle a|) + \hbar\sum_k \Omega_{bb'k}(B_k|b\rangle\langle b'| + B_k^\dagger|b'\rangle\langle b|) + \hbar\sum_k \Omega_{cc'k}(B_k|c\rangle\langle c'| + B_k^\dagger|c'\rangle\langle c|) \,, \tag{2.2}$$

where the operator B_k ($B_k^\dagger$) is the annihilation (creation) operator for the atomic reservoir modes. Equation (2.2) describes the atomic reservoir and its coupling to the atoms, where $\Omega_{\alpha\alpha'k}$ are the coupling constants between the atomic transitions $|\alpha\rangle \rightarrow |\alpha'\rangle$ and the reservoir mode k. For simplicity, from now on we consider $\Omega_{ab} = \Omega_{bc} = g$. Then, in the interaction picture, the Hamiltonian becomes

$$V_I = \hbar g e^{i\Delta_1\tau} A\,|a\rangle\langle b| + \hbar g e^{i\Delta_2\tau} A\,|b\rangle\langle c| + V_R + \text{H.c.}, \tag{2.3}$$

where τ is the time variable,

$$V_R = \hbar\sum_k \Omega_{aa'k} e^{i\Delta'_{1k}\tau} B_k\,|a\rangle\langle a'| + \hbar\sum_k \Omega_{bb'k} e^{i\Delta'_{2k}\tau} B_k\,|b\rangle\langle b'| + \hbar\sum_k \Omega_{cc'k} e^{i\Delta'_{3k}\tau} B_k\,|c\rangle\langle c'| \,, \tag{2.4}$$

$\Delta'_{1k} = \omega_a - \omega_{a'} - \omega_k$, $\Delta'_{2k} = \omega_b - \omega_{b'} - \omega_k$ and $\Delta'_{3k} = \omega_c - \omega_{c'} - \omega_k$. In describing the time evolution of the system we assume that the decay from the unprimed to primed states is an irreversible process. In this approximation the most general state of the system after the ith atom enters the cavity at time t_i is

$$|\Psi(t_i+\tau)\rangle = \sum_N \{C_{a,N,\{0\}}(t_i+\tau)|a\rangle|\{0\}\rangle + C_{b,N,\{0\}}(t_i+\tau)|b\rangle|\{0\}\rangle + C_{c,N,\{0\}}(t_i+\tau)|c\rangle|\{0\}\rangle$$
$$+\sum_k [C_{a',N,\{1_k\}}(t_i+\tau)|a'\rangle + C_{b',N,\{1_k\}}(t_i+\tau)|b'\rangle + C_{c',N,\{1_k\}}(t_i+\tau)|c'\rangle]|\{1_k\}\rangle\}\,|N\rangle, \tag{2.5}$$

where $|\{0\}\rangle$ stands for the field reservoir vacuum, $|\{1_k\}\rangle$ for a state in which all reservoir modes are empty but for one photon in mode k, and $|N\rangle$ for N photons in the resonant cavity mode. Substituting this state into the Schrödinger equation, we obtain differential equations for the expansion coefficients

$$\dot{C}_{a,N,\{0\}}(t_i+\tau) = -ige^{i\Delta_1\tau}\sqrt{N+1}\,C_{b,N+1,\{0\}}(t_i+\tau) -i\sum_k \Omega_{aa'k}e^{i\Delta'_{1k}\tau}C_{a',N,\{1_k\}}(t_i+\tau), \tag{2.6a}$$

$$\dot{C}_{b,N+1,\{0\}}(t_i+\tau) = -ige^{-i\Delta_1\tau}\sqrt{N+1}\,C_{a,N,\{0\}}(t_i+\tau) -ige^{i\Delta_2\tau}\sqrt{N+2}\,C_{c,N+2,\{0\}}(t_i+\tau) -i\sum_k \Omega_{bb'k}e^{i\Delta'_{2k}\tau}C_{b',N+1,\{1_k\}}(t_i+\tau), \tag{2.6b}$$

$$\dot{C}_{c,N+2,\{0\}}(t_i+\tau) = -ige^{-i\Delta_2\tau}\sqrt{N+2}\,C_{b,N+1,\{0\}}(t_i+\tau) -i\sum_k \Omega_{cc'k}e^{i\Delta'_{3k}\tau}C_{c',N+2,\{1_k\}}(t_i+\tau), \tag{2.6c}$$

$$\dot{C}_{a',N,\{1_k\}}(t_i+\tau) = -i\Omega_{aa'k}e^{-i\Delta'_{1k}\tau}C_{a,N,\{0\}}(t_i+\tau), \tag{2.6d}$$

$$\dot{C}_{b',N+1,\{1_k\}}(t_i+\tau) = -i\Omega_{bb'k}e^{-i\Delta'_{2k}\tau}C_{b,N+1,\{0\}}(t_i+\tau), \tag{2.6e}$$

$$\dot{C}_{c',N+2,\{1_k\}}(t_i+\tau) = -i\Omega_{cc'k}e^{-i\Delta'_{3k}\tau}C_{c,N+2,\{0\}}(t_i+\tau), \tag{2.6f}$$

where the overdot represents the time derivative $\frac{d}{d\tau}$ and t_i is the time at which the ith atom enters the cavity. Now, integrating (2.6d)–(2.6f), using the resulting expressions into (2.6a)–(2.6c), and performing the Weisskopf-Wigner approximation [12,13] we obtain

$$\dot{C}_{a,N,\{0\}}(t_i+\tau) = -\frac{\gamma_a}{2}\,C_{a,N,\{0\}}(t_i+\tau) -ige^{i\Delta_1\tau}\sqrt{N+1}\,C_{b,N+1,\{0\}}(t_i+\tau), \tag{2.7a}$$

$$\dot{C}_{b,N+1,\{0\}}(t_i+\tau) = -\frac{\gamma_b}{2}\,C_{b,N+1,\{0\}}(t_i+\tau) -ige^{-i\Delta_1\tau}\sqrt{N+1}\,C_{a,N,\{0\}}(t_i+\tau) -ige^{i\Delta_2\tau}\sqrt{N+2}\,C_{c,N+2,\{0\}}(t_i+\tau), \tag{2.7b}$$

$$\dot{C}_{c,N+2,\{0\}}(t_i+\tau) = -\frac{\gamma_c}{2}\,C_{c,N+2,\{0\}}(t_i+\tau) -ige^{-i\Delta_2\tau}\sqrt{N+2}\,C_{b,N+1,\{0\}}(t_i+\tau), \tag{2.7c}$$

where $\gamma_j = 2\pi\mathcal{D}(\omega_j-\omega_{j'})|\Omega_{jj'}(\omega_j-\omega_{j'})|^2$ ($j=a,b,c$) are the spontaneous-emission decay rates from levels a, b, and c, respectively, and $\mathcal{D}(\Omega)$ is the density of modes of the atomic reservoir. In order that two photons be emitted almost simultaneously in the cascade transition $|a\rangle \to |b\rangle \to |c\rangle$ the intermediate state $|b\rangle$ should never be really substantially populated. In addition, we assume that these two photons are resonant with the transition $|a\rangle \to |c\rangle$. The last condition implies that $\Delta_1 = -\Delta_2 \equiv \Delta$. The first condition requires that the detuning Δ be much larger than the Rabi frequencies involved. In this situation and in the limit of infinite lifetimes the population of the upper and lower atomic levels oscillates with the effective two-photon Rabi frequency [4]

$$\Omega_N = (2N+3)\frac{g^2}{\Delta}, \tag{2.8}$$

when there are N photons inside the cavity. We now obtain an expression for the gain, valid when the lifetimes are finite. When the atomic lifetimes are much larger than the transit time $t_{\rm int}$ we recover the usual expression for the gain in the two-photon micromaser [4]. In the opposite case we obtain an expression for the laser gain. Our general expression will be important in understanding how certain properties of the micromaser due to the quantized character of the field may be smoothed out by the interaction of the atoms with its reservoir. We assume that the atoms enter in the cavity one by one in the upper level $|a\rangle$, that is, $C_{a,N,\{0\}}(t_i) = 1$ and $C_{b,N+1,\{0\}}(t_i) = C_{c,N+2,\{0\}}(t_i) = 0$ and spend a time $t_{\rm int}$ inside the cavity.

The system of differential equations (2.7) can be solved using Laplace transforms. A simpler expression connecting the amplitudes at time t_i and $t_i + t_{\rm int}$ may then be obtained in the limit $\gamma_a, \gamma_b, \gamma_c < \Omega_N \ll \Delta$,

$$C_{a,N,\{0\}}(t_i+\tau)$$
$$\approx -C_{a,N,\{0\}}(t_i)e^{i\Omega_N\tau}e^{-\gamma_{ac}\frac{\tau}{2}}$$
$$\times\left\{\frac{(\delta_{ac}-ig^2/\Delta)\sin\left(\frac{\tau}{2}\sqrt{\Omega_N^2-\delta_{ac}^2+2i\delta_{ac}\frac{g^2}{\Delta}}\right)}{\sqrt{\Omega_N^2-\delta_{ac}^2+2i\delta_{ac}\frac{g^2}{\Delta}}}\right.$$
$$\left.-\cos\left(\frac{\tau}{2}\sqrt{\Omega_N^2-\delta_{ac}^2+2i\delta_{ac}\frac{g^2}{\Delta}}\right)\right\}, \quad (2.9)$$

$$C_{b,N+1,\{0\}}(t_i+\tau)\approx 0, \quad (2.10)$$

$$C_{c,N+2,\{0\}}(t_i+\tau)\approx C_{a,N,\{0\}}(t_i)e^{-i\Omega_N\tau}e^{-\gamma_{ac}\frac{\tau}{2}}$$
$$\times\frac{2i(g^2/\Delta)\sqrt{(N+1)(N+2)}}{\sqrt{\Omega_N^2-\delta_{ac}^2+2i\delta_{ac}\frac{g^2}{\Delta}}}$$
$$\times\sin\left(\frac{\tau}{2}\sqrt{\Omega_N^2-\delta_{ac}^2+2i\delta_{ac}\frac{g^2}{\Delta}}\right), \quad (2.11)$$

where $\delta_{ac}=[\gamma_a-\gamma_c)/2$ and $\gamma_{ac}=(\gamma_a+\gamma_c)/2$. The time evolution of the reduced density operator for the radiation field may then be obtained by taking the trace over the atomic variables of the full density matrix. As the atoms enter the cavity in the upper state, only the diagonal elements $\pi_N\equiv\rho_{N,N}$ in the number basis will be different from zero. The diagonal elements $\pi_N(t_i+t_{\rm int})$ describing the new state of the field after the passage of one atom through the cavity during the time $t_{\rm int}$ are related to the diagonal elements describing the old state of the field, before the atom entered the cavity, by the gain operator M,

$$\pi_N(t_i+t_{\rm int})=[M\pi(t_i)]=(1-\beta_{N+2})\ \pi_N(t_i)$$
$$+\beta_N\ \pi_{N-2}(t_i)\equiv\Gamma_N, \quad (2.12)$$

where

$$\beta_{N+2}=\frac{(N+1)(N+2)}{2N_\gamma^2(X_N^2+Y_N^2)}\left(\frac{1-r_\gamma^2-4X_N^2}{(1+r_\gamma)^2-4X_N^2}\left\{\exp\left[-\frac{1}{2}\gamma_a t_{\rm int}(1+r_\gamma)\right]\cosh(\gamma_a t_{\rm int}X_N)-1\right\}\right.$$
$$-4\frac{r_\gamma X_N}{(1+r_\gamma)^2-4X_N^2}\exp\left[-\frac{1}{2}\gamma_a t_{\rm int}(1+r_\gamma)\right]\sinh(\gamma_a t_{\rm int}X_N)$$
$$-\frac{1-r_\gamma^2+4Y_N^2}{(1+r_\gamma)^2+4Y_N^2}\left\{\exp\left[-\frac{1}{2}\gamma_a t_{\rm int}(1+r_\gamma)\right]\cos(\gamma_a t_{\rm int}Y_N)-1\right\}$$
$$\left.+4\frac{r_\gamma Y_N}{(1+r_\gamma)^2+4Y_N^2}\exp\left[-\frac{1}{2}\gamma_a t_{\rm int}(1+r_\gamma)\right]\sin(\gamma_a t_{\rm int}Y_N)\right), \quad (2.13)$$

and

$$X_N=\frac{1}{\sqrt{2}}\left(\left\{\left[\left(\frac{2N+3}{2N_\gamma}\right)^2-\left(\frac{1-r_\gamma}{2}\right)^2\right]^2+\left(\frac{1-r_\gamma}{2N_\gamma}\right)^2\right\}^{1/2}+\left(\frac{r_\gamma-1}{2}\right)^2-\left(\frac{2N+3}{2N_\gamma}\right)^2\right)^{1/2}, \quad (2.14)$$

$$Y_N=\frac{1}{\sqrt{2}}\left(\left\{\left[\left(\frac{2N+3}{2N_\gamma}\right)^2-\left(\frac{1-r_\gamma}{2}\right)^2\right]^2+\left(\frac{1-r_\gamma}{2N_\gamma}\right)^2\right\}^{1/2}-\left(\frac{r_\gamma-1}{2}\right)^2+\left(\frac{2N+3}{2N_\gamma}\right)^2\right)^{1/2}, \quad (2.15)$$

where $r_\gamma=\gamma_c/\gamma_a$ is the ratio between the upper and the lower levels widths and

$$N_\gamma=\frac{1}{2}\frac{\gamma_a}{g^2/\Delta}. \quad (2.16)$$

The quantity N_γ is proportional to the ratio between the rate of atomic decay γ_a and the effective two-photon coupling constant g^2/Δ and therefore it indicates how important atomic decay is compared to Rabi oscillations. In (2.12) the first term on the right-hand side is the probability $\pi_N(t_i)$ of finding N photons in the cavity mode at time t_i multiplied by the probability $(1-\beta_{N+2})$ that the atom remains in the upper level a. The second term is the probability $\pi_{N-2}(t_i)$ of finding $N-2$ photons in the cavity mode at the time t_i multiplied by the probability β_N that the atom emits two photons. It is interesting to examine some limiting cases of (2.13). In the limit where the atoms have a lifetime much larger than the interaction time $t_{\rm int}$, we reobtain the usual expression [4] for the gain of the degenerate two-photon micromaser

$$\beta_{N+2}=\frac{4(N+1)(N+2)}{(2N+3)^2}\sin^2\left(\frac{1}{2}\Omega_N t_{\rm int}\right). \quad (2.17)$$

For the opposite case in which the interaction time of the atoms with the field inside the cavity is much larger than the atomic lifetimes, we obtain an expression for the gain of a one atom two-photon laser

$$\beta_{N+2} = \frac{r_\gamma(r_\gamma+1)}{r_\gamma(r_\gamma+1)^2 - \left(\frac{1-r_\gamma}{2N_\gamma^2}\right)^2 + \left(\frac{(r_\gamma+1)(2N+3)}{2N_\gamma}\right)^2} \times \frac{2(N+1)(N+2)}{2N_\gamma^2}, \tag{2.18}$$

which agrees with the expression obtained in [15] for the case where both upper and lower level decay rates are equal.

As far as we know, this is the first time such an expression is derived for different decay rates. We notice that, as the gain saturates, one atom two-photon lasers do lase, according to our model. If $\gamma_c = \gamma_a$ ($r_\gamma = 1$), we recover the expression obtained in Ref. [6]

$$\beta_{N+2} = 2\frac{(N+1)(N+2)}{(2N+3)^2+(2N_\gamma)^2} \times \left[1 - e^{-\gamma t_{\rm int}}\left(\cos(\Omega_N t_{\rm int}) - \frac{2N_\gamma}{(2N+3)}\sin(\Omega_N t_{\rm int})\right)\right]. \tag{2.19}$$

As we have mentioned before we assume that field dissipation may be treated independently of the gain. The damping process of a field inside a cavity may be described by [13]

$$(\dot\rho)_{\rm loss} = L\rho = \frac{1}{2t_{\rm cav}}(N_T+1)(2A\rho A^\dagger - A^\dagger A\rho - \rho A^\dagger A) + \frac{1}{2t_{\rm cav}}N_T(2A^\dagger\rho A - AA^\dagger\rho - \rho AA^\dagger), \tag{2.20}$$

where N_T is the mean photon number for a cavity in equilibrium at temperature T. Both the finite temperature and finite lifetimes introduce fluctuations in the system. As we are interested primarily in studying the influence of finite lifetimes we set $N_T = 0$. Therefore the change in the reduced density operator for the field due to the passage of the ith atom is given by

$$\rho(t_{i+1}) = e^{L\Delta t_i}\, M\rho(t_i), \tag{2.21}$$

where M is the gain operator whose action in the populations is given by (2.12), $\Delta t_i = t_{i+1} - t_i$, and L is given by (2.20) with $N_T = 0$. In the analysis of noise it is also important to consider the statistics of the pumping mechanism. In this paper we consider the Poissonian and regular pumping statistics [16] cases. In the Poissonian case, the distribution of time intervals Δt_i is given by $r\exp(-r\Delta t_i)$, where r is the average pumping rate [9]. Taking the statistical average of (2.21) over this distribution, we find for the change in the mean field operator (over the average interval of time between two atoms of $t_{\rm at} = 1/r$)

$$\bar\rho(t+t_{\rm at}) = (1 - L/r)^{-1} M\bar\rho(t). \tag{2.22}$$

From (2.20) and (2.22) we obtain for the average change in the photon population during $t_{\rm at}$

$$\bar\pi_N(t_{i+1}) = (1-\beta_{N+2})\,\bar\pi_N(t_i) + \beta_N\bar\pi_{N-2}(t_i) + \frac{1}{N_{\rm ex}}\Big[(N+1)\bar\pi_{N+1}(t_{i+1}) - N\bar\pi_N(t_{i+1})\Big], \tag{2.23}$$

where $N_{\rm ex} = rt_{\rm cav} = t_{\rm cav}/t_{\rm at}$ is the average number of atoms that cross the cavity during the lifetime $t_{\rm cav}$ of a photon inside the cavity.

For regular pumping, the time interval is $\Delta t_i = t_{\rm at} =$ const and another difference equation is obtained. Defining $x_\tau = \tau/2t_{\rm cav}$ and

$$\tilde\rho(x_\tau) = \exp(x_\tau A^\dagger A)\rho(x_\tau)\exp(x_\tau A^\dagger A) \tag{2.24}$$

for $N_T = 0$, Equation (2.20) becomes

$$\frac{d\tilde\rho}{dx_\tau} = e^{2x_\tau}K\tilde\rho, \tag{2.25}$$

where $K\rho = 2A\rho A^\dagger$. Equation (2.25) can be integrated easily, yielding

$$\tilde\rho(x_t + x_\tau) = \exp\{(\exp 2x_\tau - 1)K\}\,\tilde\rho(x_t), \tag{2.26}$$

where $x_t = t/2t_{\rm cav}$. As before, we treat the gain and the loss independently. Therefore the total change in the density operator after the passage of one atom is

$$\begin{aligned}\rho(t+t_{\rm at}) &= \exp(-\delta A^\dagger A)\exp\{(\exp 2\delta - 1)K\} \times\rho(x_t)\exp(-\delta A^\dagger A)\\ &= \sum_{j=0}^{\infty}\frac{(1-e^{-2\delta})^j}{j!}e^{-\delta A^\dagger A} \times (A)^j M\rho(t)(A^\dagger)^j e^{-\delta A^\dagger A},\end{aligned} \tag{2.27}$$

where

$$\delta = \frac{t_{\rm at}}{2t_{\rm cav}} = \frac{1}{2N_{\rm ex}}. \tag{2.28}$$

Then taking into account (2.12) and (2.27), the diagonal elements of the field reduced matrix after an atom has passed through the cavity can be written as

$$\pi_N(t+t_{\rm at}) = e^{-2\delta N}\sum_{j=0}^{\infty}\frac{(N+j)!}{N!j!}\,(1-e^{-2\delta})^j\Gamma_{j+N}(t), \tag{2.29}$$

where Γ_N is given by (2.12). We may then obtain the steady-state photon distribution starting from the vacuum and applying (2.29) successively.

We are now ready to discuss the predictions of this model. We start by showing how the physics of the system described above changes as we go from a micromaser to a laser by changing the parameters of our model.

III. FROM MICROMASERS TO LASERS

The micromaser is a dynamic system away from thermodynamic equilibrium and it needs to be pumped with energy. This is done by feeding excited atoms into the cavity. The effectiveness of this pumping will depend on how many of these atoms go through the cavity during the average time the cavity radiation field loses one photon of frequency ω, on the coupling strength of the two-photon transition, and on the transit time of an atom through the cavity. This leads us to consider $\varphi_{\rm int} = N_{\rm ex}(2g^2/\Delta)t_{\rm int}$ as a pumping parameter.

Lasers operate in the visible spectrum where atomic lifetimes are small compared to transit times of the atoms through the cavity. Therefore in the limit of large $\gamma_a t_{\rm int}$ our two-photon micromaser model will describe a two-photon laser. This is illustrated in Fig. 2, which shows the probability of finding the atoms in the lower state as they leave the cavity, which is proportional to the mean photon number [6], as a function of the pumping parameter, for fixed $N_{\rm ex} = 15$ and $\gamma_a = \gamma_c = 0.02g^2/\Delta$ ($N_\gamma = 0.1, r_\gamma = 1$). This result was obtained by a numerical calculation of the dynamic steady state and in the case of Poissonian pumping statistics.

For large $N_{\rm ex} = t_{\rm cav}/t_{\rm at}$ we expect that the important contributions for the density operator ρ occur for large N. Therefore we may define a continuous function $\rho(n,\tau) \equiv \pi_N(t)$ of the normalized photon number $n = N/N_{\rm ex}$ and normalized time $\tau = t/t_{\rm cav}$. In Ref. [4] a Fokker-Planck equation for such a function was derived in the limit of infinite lifetimes. We follow the same procedure in the case of finite lifetimes. We first approximate the time difference Eq. (2.23) to a time differential equation by multiplying it by $r = 1/t_{\rm at}$ and substituting the rate of the population variation by a time derivative and then we make an expansion of $\rho(n,\tau)$ up to second order in the variable $\delta = 1/(2N_{\rm ex})$. We obtain

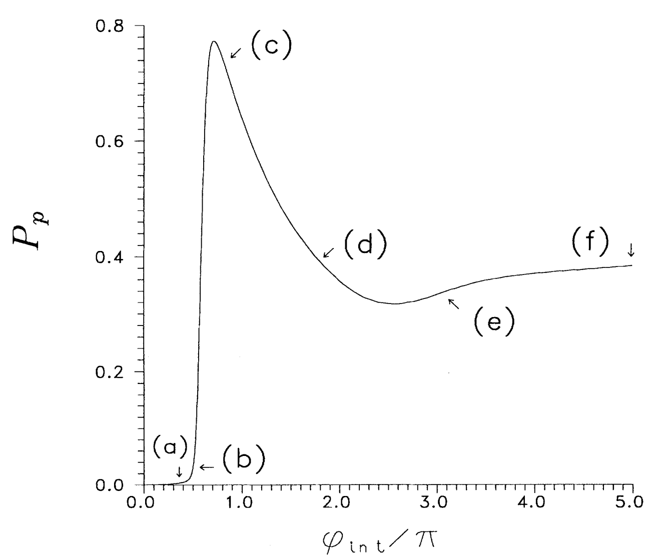

FIG. 2. Probability of detecting an atom in energy level $|c\rangle$ as it exits the cavity as a function of the pumping parameter for $N_{\rm ex} = 15$. In Fig. 3 we show the effective potential at values of $\varphi_{\rm int}$ indicated by (a)–(f). The pumping statistics is Poissonian and $\gamma_a = \gamma_c = 0.2g^2/\Delta$ ($N_\gamma = 0.1$ and $r_\gamma = 1$).

$$\frac{\partial}{\partial\tau}\rho(n,\tau) = -\delta\frac{\partial}{\partial n}\left[a_1(n)\rho(n,\tau)\right] + \frac{\delta^2}{2}\frac{\partial^2}{\partial n^2}\left[a_2(n)\rho(n,\tau)\right] + \mathcal{O}\left(\delta^3\right), \qquad (3.1)$$

where

$$a_1(n) = 2\left[\beta(\delta=0) + \delta\left.\frac{\partial\beta}{\partial\delta}\right|_{\delta=0} - n\right] \qquad (3.2a)$$

and

$$a_2(n) = 4\beta(\delta=0) + 2n. \qquad (3.2b)$$

We can draw an interesting analogy with thermodynamics if we write the dynamic steady-state photon distribution $\rho^S(n)$ calculated from the Fokker-Planck equation in the form of a Boltzmann distribution [4]

$$\rho^S(n) = \exp\left[-2V_F(n)/\delta\right], \qquad (3.3)$$

where

$$V_F(n) = -\int_0^n \frac{a_1(n')}{a_2(n')}dn' + \frac{\delta}{2}\ln a_2(n) + C \qquad (3.4)$$

with C the normalization constant. We can think of the argument of the exponential as the ratio between an effective potential V_F and an energy associated with random fluctuations δ. As in thermodynamics, the system tends to stay in the wells of the potential with the random fluctuations moving it around. Therefore, when the system is in a local minimum, if the fluctuations are large enough (i.e., if the energy associated with them is large enough), the system will eventually move to the global minimum.

In Fig. 3, at some strategic values of the pumping parameter, we also display plots of the effective potential as a function of the normalized photon number n. This was calculated numerically at the dynamic steady state and for the same parameters ($N_{\rm ex} = 15$, $N_\gamma = 0.1$, and $r_\gamma = 1$) used. We notice that for small values of the pumping parameter [Fig. 3(a)], the effective potential has only one well at the origin. This corresponds to the situation below threshold. Then, as the pumping parameter increases, another well appears [Fig. 3(b)] away from the origin and the mean photon number grows quite abruptly. When the depth of this well becomes approximately the same as the one at the origin [Fig. 3(c)], quantum fluctuations can drive the system from the well at the origin to this additional well and we reach threshold. As the pumping parameter increases even more, the well away from the origin starts moving towards the origin [Fig. 3(d)], becomes deeper and deeper, other wells appear and the mean photon number decreases [Figs. 3(e) and 3(f)]. This corresponds to the situation above threshold. The multiple wells reflect the fact that the photon distribution of the micromaser can have more than two peaks. For really large values of the pumping parameter, most wells become shallower and shallower and disappear, except for two. One of these surviving wells is at the origin and one is away from the origin. Depending on the values of the other parameters, sometimes only the well away from the origin survives. This corresponds to the two-photon laser limit and it reflects the fact that the photon distribution has at most two peaks [17].

IV. TRAPPING STATES

Previous theories of the micromaser [4,7], where atomic damping has been neglected, make a very interesting prediction. For certain values of the pumping parameter, every atom that enters the cavity when there are N photons in the cavity mode will exit in the excited state. This is usually referred to as an N-photon trapping state [7] because the cavity field stops growing after it acquires N photons.

Both the Jaynes-Cummings revivals [18] and the trapping states are a signature of the discrete quantum nature of the field. If the field energy could assume any continuous value, neither trapping states nor revivals would exist. The similarities, however, end there. Jaynes-Cummings revivals are extremely sensitive to cavity dissipation and they decay much faster than the field energy [19]. Atomic losses, on the other hand, do not have such a strong effect on them [20]. Revivals decay at the same

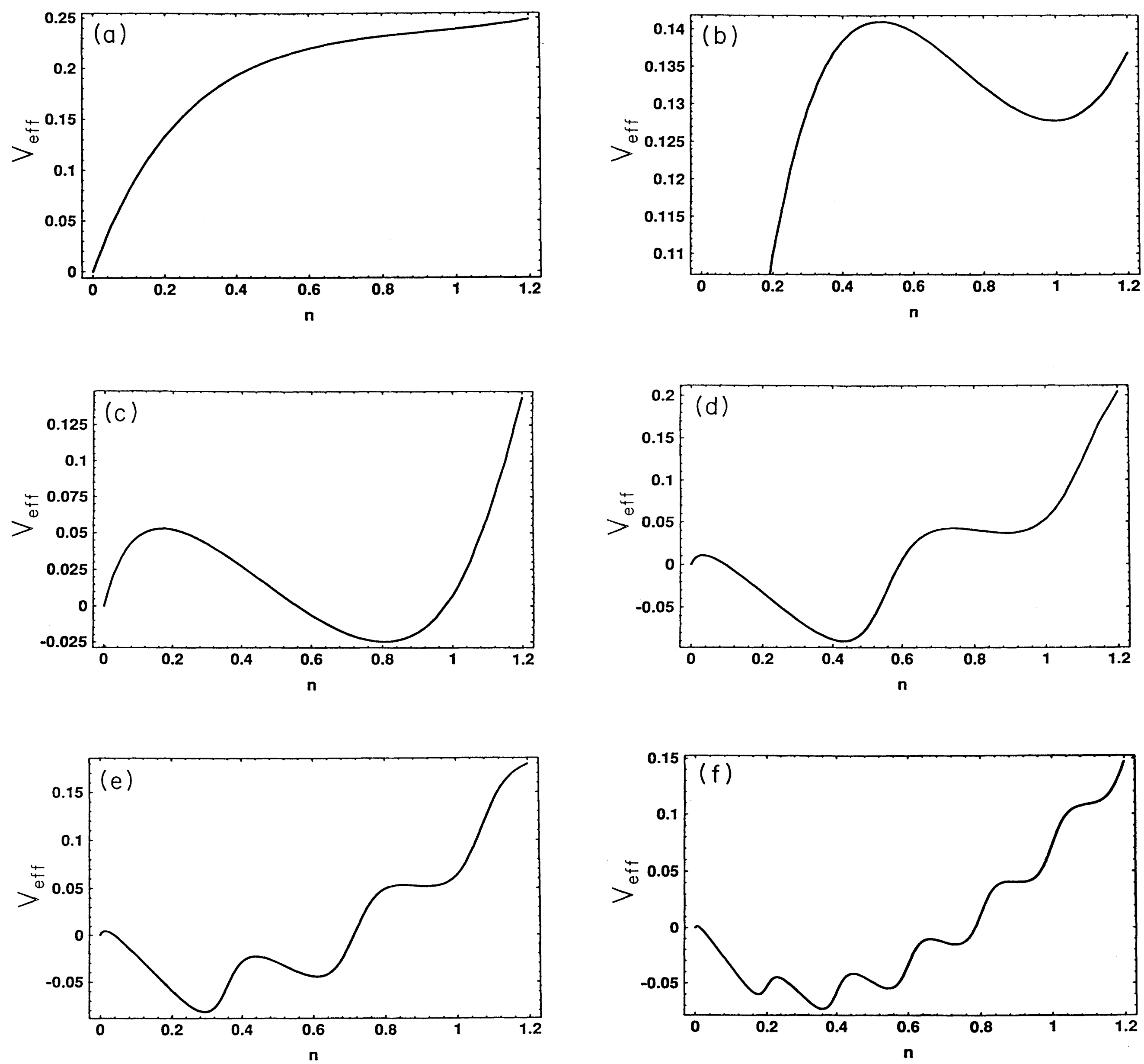

FIG. 3. Effective potential for (a) $\varphi_{\rm int} = 0.4\pi$ (below threshold), (b) $\varphi_{\rm int} = 0.5\pi$ (close to threshold), and (c) $\varphi_{\rm int} = 0.8\pi$ (above threshold). The extra well becomes deeper than the one at the origin. (d) $\varphi_{\rm int} = 1.8\pi$ (another well appears), (e) $\varphi_{\rm int} = 2.8\pi$ (multiple wells), and (f) $\varphi_{\rm int} = 5\pi$ (the multiple wells become shallower).

rate atomic energy does. Trapping states, unlike revivals, are extremely sensitive to atomic decay. Figure 4 shows how sensitive to atomic decay trapping states are. We plot the dynamic steady-state probability of finding the atom in the lower energy level as it exits the cavity (which is proportional to the average number of photons) as a function of the pumping parameter for $N_{\text{ex}} = 15$. This was computed numerically from the master equation we derived for the two-photon micromaser with atomic losses and regular pumping. The full curve corresponds to no atomic decay. The dashed curve corresponds to the case where the decay rate of the upper energy level is 0.02 of the effective two-photon coupling constant g^2/Δ and the decay rate of the lower energy level is 5 times larger.

We notice that the average photon number goes to zero on the lower curve when the pumping parameter is 20π. This corresponds to a $N = 0$ trapping state, which is no longer present on the upper curve. The sensitivity of trapping states to atomic losses has been noted previously in a different context. It was shown [5] that trapping states disappear completely in one-photon micromasers even when the average atomic decay time is much longer than the transit time through the cavity. There is, however, an important difference between the way atomic decay affects trapping states in one-photon and two-photon micromasers.

In a one-photon micromaser, trapping states are sensitive to atomic decay of the lower energy level only. As we have mentioned above, trapping states depend on the atom not leaving any photons in the cavity after the photon distribution has reached a certain photon number. The detection (in principle) of atomic decay serves as a measurement of which state the atom was in and that is why it affects trapping states. Consider a two-level atom entering the cavity in the excited state. For an N trapping state to develop, the atom has to perform complete Rabi cycles when it is inside the cavity so that it can exit the cavity in the upper state without leaving photons in the cavity mode. Now, if the atom decays from the lower state when it is in the cavity, it has to have left its energy in the cavity mode (because it entered the cavity in the excited state), destroying the trapping state. Atomic decay works here as a measurement of atomic energy. If this measurement is made when the atom is performing Rabi oscillations and is in a quantum superposition of the two energy states, there will be a finite probability of finding the atom in the lower energy state. Because the field becomes entangled with the atom through their interaction, detecting the atom in the lower energy level collapses the field into a state where the field has gained some extra energy.

We notice that according to the argument given above, trapping states would be affected only by the decay of the lower energy level. This is, in fact, the case in one-photon micromasers. We have found, however, that in two-photon micromasers, trapping states are sensitive to the decay of the upper energy level as well as that of the lower.

An example of the sensitivity of the trapping states to the decay of the upper level can be seen in Fig. 5, where we plot the average number of photons as a function of the pumping parameter for the case where the lower level is metastable (i.e., $\gamma_c = 0$). We plot three curves, all of them for regular pumping statistics and $N_{\text{ex}} = 15$, so that there is a trapping state at $\varphi_{\text{int}} = 20\pi$ in the ideal case of no atomic decay as in Fig. 4. The dotted curve

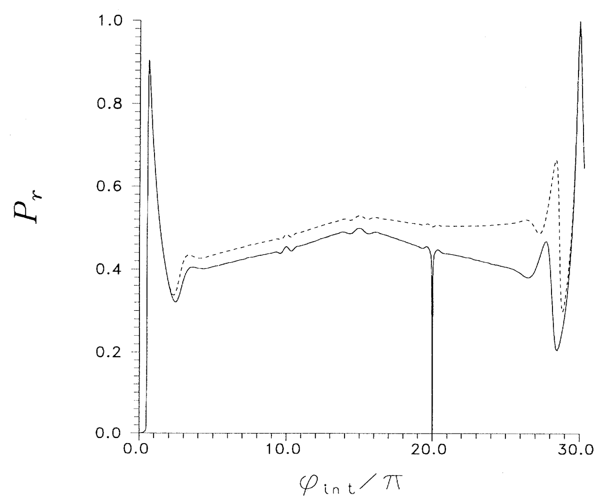

FIG. 4. Probability of detecting an atom exiting the cavity in level $|c\rangle$ as a function of the pumping parameter in the steady state for $N_{\text{ex}} = 15$ and regular pumping statistics. The full line shows a micromaser without atomic decay. The dashed line corresponds to $N_\gamma = 0.01$ and $r_\gamma = 5$ (notice that the trapping dip at $\varphi_{\text{int}} = 20\pi$ disapears).

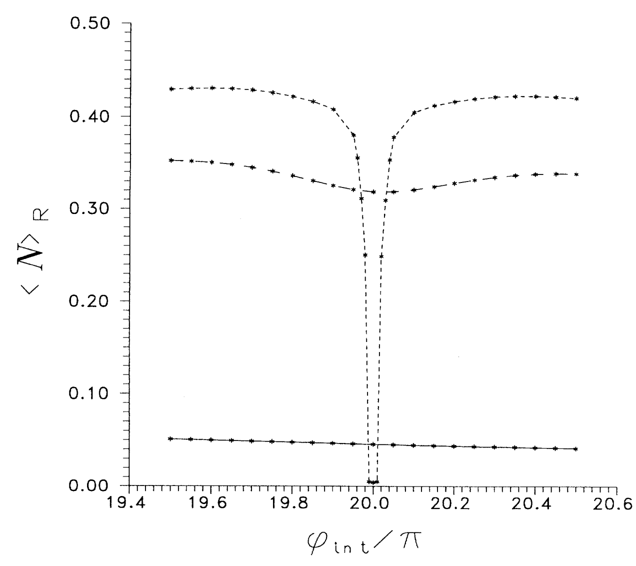

FIG. 5. Average number of photons as a function of the pumping parameter for $\gamma_c = 0$, $N_{\text{ex}} = 15$, and regular pumping statistics. The full curve correspond to the case where $N_\gamma = 1$, the dashed curve to $N_\gamma = 0.1$, and the dotted curve to $N_\gamma = 0.01$. We notice that the trapping state that exists at $\varphi_{\text{int}} = 20\pi$ in the case of no atomic decay is not an exact trapping state even when the decay rate of the upper level is very small (dotted curve) and disappears completely for larger decay rates (dashed and full curves).

shows the case where the decay rate of the upper level is 0.02 of the effective two-photon coupling constant (i.e., $N_\gamma = 0.01$). The dashed curve corresponds to the case where the decay rate of the upper level is 0.2 of the effective two-photon coupling constant (i.e., $N_\gamma = 0.1$) and the full curve, to the case where the decay rate is twice the effective two-photon coupling constant (i.e., $N_\gamma = 1$). We notice that even when the decay rate of the upper level is quite small (dotted curve) the trapping state is already affected because the average number of photons does not vanish completely at $\varphi_{\rm int} = 20\pi$. As the decay rate of the upper level increases, the trapping states disappears, leaving no trace when $N_\gamma = 1$.

We can demonstrate analytically the sensitivity of the trapping states on the decay rate of the upper level by taking the limit of the conditional probability of emitting two photons β_N, given by Eq. (2.13), when $\gamma_c \to 0$. After some algebra, we find

$$\beta_N = \frac{1}{2}\frac{(N+1)(N+2)}{(A_N^2+B_N^2)N_\gamma^2}e^{-\frac{N_\gamma}{2N_{\rm ex}}\varphi_{\rm int}} \times \left[\cosh\left(A_N\frac{N_\gamma}{N_{\rm ex}}\varphi_{\rm int}\right) - \cos\left(B_N\frac{N_\gamma}{N_{\rm ex}}\varphi_{\rm int}\right)\right], \tag{4.1}$$

where

$$A_N = \left(\frac{1}{2}\left\{\frac{1}{4} - \left(\frac{2N+3}{2N_\gamma}\right)^2 + \sqrt{\left[\frac{1}{4} - \left(\frac{2N+3}{2N_\gamma}\right)^2\right]^2 + \left(\frac{1}{2N_\gamma}\right)^2}\right\}\right)^{1/2} \tag{4.2}$$

and

$$B_N = \left(\frac{1}{2}\left\{\left(\frac{2N+3}{2N_\gamma}\right)^2 - \frac{1}{4} + \sqrt{\left[\frac{1}{4} - \left(\frac{2N+3}{2N_\gamma}\right)^2\right]^2 + \left(\frac{1}{2N_\gamma}\right)^2}\right\}\right)^{1/2}. \tag{4.3}$$

We see that, because the term in square brackets in Eq. (4.1) involves the difference between a hyperbolic cosine and a cosine, β_N will vanish only when $\varphi_{\rm int} = 0$ unless $A_N N_\gamma/N_{\rm ex} = 0$. From Eq. (4.2), we see that $A_N N_\gamma/N_{\rm ex} = 0$ only when $\gamma_a = 0$, so we conclude that β_N never vanishes for $\varphi_{\rm int} > 0$ when the upper level is not metastable (i.e., $\gamma_a \neq 0$). Because β_N is the conditional probability of the atom emitting two photons given that there are N photons in the cavity, the fact that β_N does not vanish for any nonzero value of $\varphi_{\rm int}$ in this case shows there can be no trapping state when $\gamma_a \neq 0$.

A most obvious difference between two-photon and one-photon micromasers is that the former employs three-level atoms, not two-level atoms as does the latter. It is tempting to think that this is the reason why trapping states are sensitive to the decay of the upper energy level. However, when the detuning is very large and the atoms enter the cavity in the excited state, the intermediate level is never populated and takes part in the process only through virtual one-photon transitions off resonance with the cavity mode. These virtual transitions produce a Stark shift in the atomic energy levels. So our three-level atoms are equivalent to two-level atoms performing two-photon transitions plus the Stark shift [14]. It is because of the Stark shift that the decay rate of the upper energy level can affect trapping states in two-photon micromasers. In fact, we were able to reproduce all our results using the following effective Hamiltonian in the interaction picture [21]

$$H_I = \hbar\lambda_2(A^\dagger A + 1)|a\rangle\langle a| + \hbar\lambda_1 A^\dagger A|c\rangle\langle c| + \hbar\lambda\left(A^2|a\rangle\langle c| + A^{\dagger 2}|c\rangle\langle a|\right) + H_R, \tag{4.4}$$

where two-level atoms couple to the field through a two-photon effective coupling, whose coupling constant we call λ, and an additional term is added to account for the Stark shift, which will depend on the constants λ_1 and λ_2. The relation between these extra parameters λ, λ_1, and λ_2 that have been introduced here and the parameters of our model will become clear during our calculation. Atomic decay is introduced again by coupling these two-level atoms to a reservoir through the term H_R in (4.4), which is given by

$$H_R = \hbar\sum_k \Omega_{aa'k}e^{i\Delta'_{1k}\tau}B_k\,|a\rangle\langle a'| + \hbar\sum_k \Omega_{cc'k}e^{i\Delta'_{3k}\tau}B_k\,|c\rangle\langle c'|\,, \tag{4.5}$$

Starting from (4.4) and performing the Weisskopf-Wigner approximation, we can write

$$\dot{C}_{a,N}(t) = -\frac{\gamma_a}{2}C_{a,N}(t) - i\lambda_2 C_{a,N}(t) - i\lambda\sqrt{(N+1)(N+2)}C_{c,N+2}(t), \tag{4.6}$$

$$\dot{C}_{c,N+2}(t) = -\frac{\gamma_c}{2}C_{c,N+2}(t) - i\lambda_1 C_{c,N+2}(t) - i\lambda\sqrt{(N+1)(N+2)}C_{a,N}(t). \tag{4.7}$$

It is not difficult to show that the solution of the above system of differential equations is given by

$$C_{a,N,\{0\}}(t_i+\tau) = -C_{a,N,\{0\}}(t_i)e^{i\Delta_N\frac{\tau}{2}}e^{-\gamma_{ac}\frac{\tau}{2}}\left\{\frac{\mu_N\sin\left(\frac{\tau}{2}\sqrt{4\lambda^2(N+1)(N+2)-(\delta_{ac}+i\Delta_N)^2}\right)}{\sqrt{4\lambda^2(N+1)(N+2)-(\delta_{ac}+i\Delta_N)^2}} - \cos\left(\frac{\tau}{2}\sqrt{4\lambda^2(N+1)(N+2)-(\delta_{ac}+i\Delta_N)^2}\right)\right\}, \tag{4.8}$$

$$C_{c,N+2,\{0\}}(t_i+\tau) = C_{a,N,\{0\}}(t_i)e^{-i\Delta_N \frac{\tau}{2}}e^{-\gamma_{ac}\frac{\tau}{2}} \times \frac{2i\lambda^2\sqrt{(N+1)(N+2)}\sin\left(\frac{\tau}{2}\sqrt{4\lambda^2(N+1)(N+2)-(\delta_{ac}+i\Delta_N)^2}\right)}{\sqrt{4\lambda^2(N+1)(N+2)-(\delta_{ac}+i\Delta_N)^2}}, \tag{4.9}$$

where $\Delta_N = \lambda_2(N+1) - \lambda_1(N+2)$ and $\mu_N = \delta_{ac} + i\Delta_N$. If $\lambda_1 = \lambda_2 = \lambda = g^2/\Delta$ Eqs. (4.8) and (4.9) reduces to (2.9) and (2.11).

If we neglect the Stark shift term in the effective Hamiltonian ($\lambda_1 = \lambda_2 = 0$) and assume a detuning $\tilde{\Delta} = 2\omega - (\omega_a - \omega_c)$, we obtain

$$\dot{C}_{a,N}(t) = -\frac{\gamma_a}{2}C_{a,N}(t) - i\lambda e^{i\tilde{\Delta}t}\sqrt{(N+1)(N+2)}C_{c,N+2}(t), \tag{4.10}$$

$$\dot{C}_{c,N+2}(t) = -\frac{\gamma_c}{2}C_{c,N+2}(t) - i\lambda e^{-i\tilde{\Delta}t}\sqrt{(N+1)(N+2)}C_{a,N}(t). \tag{4.11}$$

The solution of the above system of differential equations is given by

$$C_{a,N,\{0\}}(t_i+\tau) = C_{a,N,\{0\}}(t_i)e^{i\frac{\tilde{\Delta}}{2}\tau}e^{-\gamma_{ac}\frac{\tau}{2}}\left\{\cos\left(\frac{\tau}{2}\sqrt{4\lambda^2(N+1)(N+2)-(\delta_{ac}+i\tilde{\Delta})^2}\right) - \frac{\delta_{ac}\sin\left(\frac{\tau}{2}\sqrt{4\lambda^2(N+1)(N+2)-(\delta_{ac}+i\tilde{\Delta})^2}\right)}{\sqrt{4\lambda^2(N+1)(N+2)-(\delta_{ac}+i\tilde{\Delta})^2}}\right\}, \tag{4.12}$$

$$C_{c,N+2,\{0\}}(t_i+\tau) = C_{a,N,\{0\}}(t_i)e^{-i\frac{\tilde{\Delta}}{2}\tau}e^{-\gamma_{ac}\frac{\tau}{2}} \times \frac{2i\lambda^2\sqrt{(N+1)(N+2)}\sin\left(\frac{\tau}{2}\sqrt{4\lambda^2(N+1)(N+2)-(\delta_{ac}+i\tilde{\Delta})^2}\right)}{\sqrt{4\lambda^2(N+1)(N+2)-(\delta_{ac}+i\tilde{\Delta})^2}}. \tag{4.13}$$

From (4.12) and (4.13), we see that if $\tilde{\Delta} \neq 0$, the rates of atomic decay for the upper and the lower states will both affect trapping states. If $\tilde{\Delta} = 0$ then $\sin\left[\sqrt{4\lambda^2(N+1)(N+2)-\delta_{ac}^2}\right]$, in principle, can be zero and the condition for having trapping states can be fulfilled. However, as we see from (4.8) and (4.9), if the dynamic Stark shift is taken into account, the condition that yields trapping states cannot be fulfilled in any circumstances because Δ_N cannot vanish for all values of N and both rates of atomic decay γ_a and γ_c affect trapping states.

We can also show, through a very simple calculation, that it is really the detuning (in our case produced by the Stark shift), not the fact that it is a two-photon transition, that is making the trapping states sensitive to the decay rate of the upper energy level. Consider a two-level atom going through a single-mode cavity in resonance with the atomic transition frequency ω. The atom enters the cavity in the upper energy state at time $t = 0$ when there are N photons in the cavity mode. If we neglect cavity damping but take atomic decay, from the upper state only, into account, we find that the probability amplitude of detecting the atom in the lower state and $N+1$ photons in the cavity mode at time $t = \tau$ is given by

$$C_{b,N+1}(\tau) = \frac{\Omega_N e^{-(\gamma_a/4)\tau}}{\sqrt{\Omega_N^2 - (\gamma_a/4)^2}}\sin\left[\sqrt{\Omega_N^2 - \left(\frac{\gamma_a}{4}\right)^2}\,\tau\right] \tag{4.14}$$

for $\Omega_N > \gamma_a/4$, where γ_a is the decay rate of the upper level, $\Omega_N = g\sqrt{N+1}$ is the Rabi frequency, and g is the coupling constant between the atom and the cavity mode. We notice that for a given value of the upper energy level decay rate γ_a, it is always possible to find some values of Ω_N and τ for which $C_{b,N+1}(\tau)$ vanishes. This means that the photon distribution will not grow beyond N photons and we will have an N-photon trapping state. So, when the cavity mode is resonant with the two-level atoms, trapping states can survive atomic decay from the upper energy level as we have mentioned earlier. This result is implicit in the expression given by Zhu *et al.* [5] for the gain coefficient β, although they do not mention it explicitly in their article, nor do they discuss its significance.

Now we consider the case where the atomic transition frequency is detuned from the cavity resonance. If the detuning is Δ, the probability amplitude $C_{b,N+1}(\tau)$ is given by

$$C_{b,N+1}(\tau) = -i\Omega_N e^{-\Lambda\tau} \frac{\sin\left(\sqrt{\Omega_N^2 - \Lambda^2}\tau\right)}{\sqrt{\Omega_N^2 - \Lambda^2}}, \quad (4.15)$$

where $\Lambda = \gamma_a/4 - i(\Delta/2)$. We notice that, because of the detuning Δ, $\sqrt{\Lambda^2 - \Omega_N^2}$ is complex. This guarantees that, for $\tau > 0$, $C_{b,N+1}(\tau)$ will not vanish for any finite values of $\Lambda\tau$. So there will be no trapping states in this case.

V. STARTING TIME

The process by which two-photon micromasers start oscillating is completely different from that of one-photon micromasers [4] and we have found that atomic decay interferes with this process in a very peculiar way. If the evolution of a micromaser is analyzed as a phase transition phenomena, the threshold of a one-photon micromaser can be regarded as a second-order phase transition [22]. The threshold of the two-photon micromaser, however, is a first-order phase transition [4]. A Fokker-Planck equation approximation to the master equation of the two-photon micromaser [4] reveals that the effective potential has a well at the origin, as we have seen in Sec. III. Because of this, the two-photon micromaser starts to oscillate only when the effective potential develops another well away from the origin as deep as the one at the origin. Quantum fluctuations then allow the system to tunnel from the well at the origin to the other well. The starting time is determined by how long it takes to tunnel through. Atomic decay affects these quantum fluctuations and changes the time for an effective tunneling. The characteristic time for tunneling may be defined quantitatively in several ways. Here we define starting time for the micromaser as the time taken for π_1 to become as large as π_0 [8] in units of t_{cav}. This is a signature that the system is tunneling from the well at the origin into the well away from the origin.

In Fig. 6, we plot the starting time as a function of the pumping parameter for $N_{\text{ex}} = 15$ and for several values of γ_a and γ_c. The starting time was calculated, in the case of Poissonian pumping statistics, by iterating numerically Eq. (2.23). Curve (a) shows an ideal two-photon micromaser with no atomic decay. Curve (b) shows a two-photon micromaser where both upper and lower energy levels have the same decay rate of 0.2 of the effective two-photon coupling constant g^2/Δ. In curves (c) and (d), the upper energy level has the same decay rate as in (b); the lower energy level, however, is decaying 20 and 50 times faster than in (b), respectively.

Although curve (b) is very close to curve (a), curves (c) and (d) display much longer starting times than (a) for the same values of the pumping parameter. This suggests that reabsorption of photons plays a very important role in the starting mechanism of two-photon micromasers. In lasers, reabsorption can only hamper the starting process. In two-photon micromasers, however, it seems to be a crucial part of the starting process. In order to confirm this argument we first study the starting time when only the upper level is stable and in the opposite case

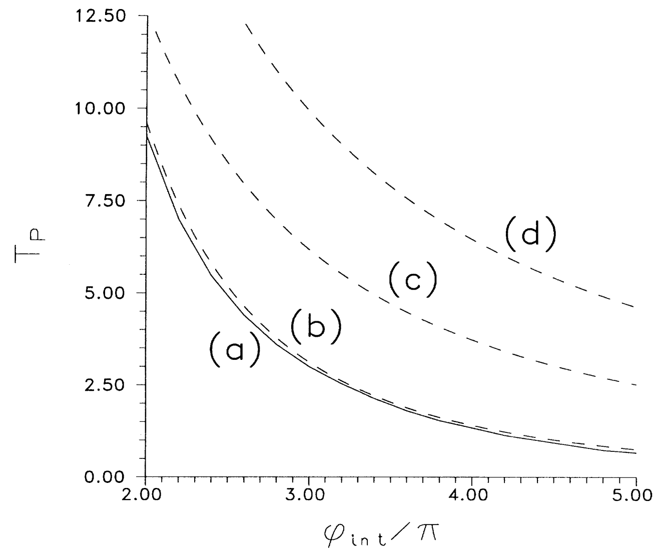

FIG. 6. Starting time as a function of the pumping parameter for $N_{\text{ex}} = 15$ and Poissonian pumping. Curve (a), micromaser with no atomic decay; curve (b), $N_\gamma = 0.1$ and $r_\gamma = 1$; curve (c), $N_\gamma = 0.1$ and $r_\gamma = 20$; and curve (d), $N_\gamma = 0.1$ and $r_\gamma = 50$.

when only the lower level is stable. Then we study how the probability of detecting an atom exiting the cavity in level $|c\rangle$ changes with r_γ.

In Fig. 7, we show the starting time as a function of the pumping parameter for two cases. The full curve shows the case where the lower energy level is metastable (i.e., its decay rate is negligible) and the decay rate of

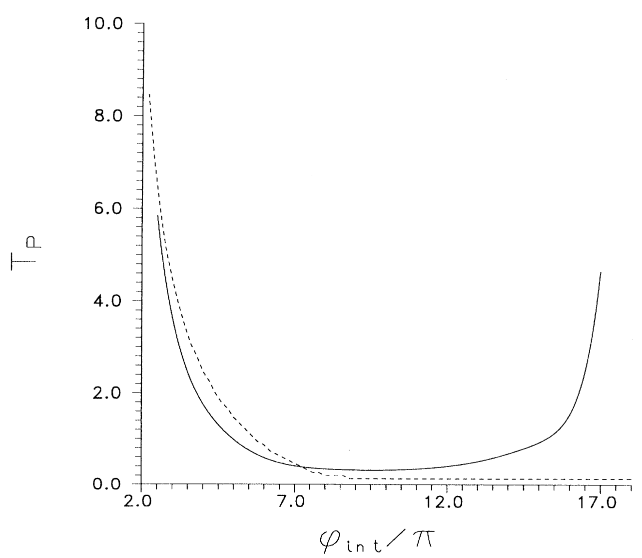

FIG. 7. Starting time as a function of the pumping parameter computed numerically for $N_{\text{ex}} = 15$ and Poissonian pumping. The full line corresponds to $\gamma_a = 2g^2/\Delta$ and $\gamma_c = 0$ ($N_\gamma = 1.0$ and $r_\gamma = 0$). The dashed line shows the reverse situation where $\gamma_c = 2g^2/\Delta$ and $\gamma_a = 0$ ($r_\gamma N_\gamma = 1.0$ and $r_\gamma^{-1} = 0$).

the upper level is twice the effective two-photon coupling constant. We notice that, for large $\varphi_{\rm int}$, the starting time always increases when $\varphi_{\rm int}$ increases. In fact, in the laser limit, the system never starts, as can be verified analytically from Eq. (2.18) by noticing that β vanishes when $\gamma_c = 0$. The dashed line shows the reverse situation where the upper energy level is metastable and the decay rate of the lower level is twice the effective two-photon coupling constant. We notice that, in the micromaser regime (i.e., when $\gamma_a t_{\rm int} = N_\gamma \varphi_{\rm int}/N_{\rm ex}$ is small), the starting time increases much more when the lower energy level decays than when the upper level decays at the same rate. However, closer to the laser regime (i.e., when the pumping parameter is large), this is reversed with the starting time actually diverging when only the upper level decays and decreasing when only the lower level decays. As we mentioned above, we can verify the divergence of the starting time in the laser limit when the lower state is metastable by taking the limit of (2.18) for $\gamma_c \to 0$ and realizing that the gain coefficient vanishes in this case. The reason why there is no gain is that more photons are reabsorbed than emitted when $\gamma_c = 0$. This point of view is also confirmed if we examine the dynamic steady state. In Fig. 8, we plot the probability P of finding the atom in the lower state when it leaves the cavity as a function of the pumping parameter for regular pumping statistics. There are two curves in Fig. 8. The upper energy level has the same decay rate in both of them ($\gamma_a = 0.2g^2/\Delta$), but the lower energy level decays faster in the full curve ($r_\gamma = 50$) than in the dashed one ($r_\gamma = 10$). We notice that the system has to be pumped harder to get to threshold for increased values of the decay rate of the lower level. So reabsorption is important in the starting process.

We have also investigated the influence of the pumping statistics on the starting time. Figure 9 shows plots of the starting time as a function of the pumping parameter for different rates of atomic decay for both Poissonian and regular pumping statistics computed numerically for $N_{\rm ex} = 15$. The full curves show the case where the decay rates of $|a\rangle$ and $|c\rangle$ are both equal to 0.2 of the effective two-photon coupling constant ($N_\gamma = 0.1$ and $r_\gamma = 1$). In the dashed curves, the decay rate of $|a\rangle$ is the same as in the full curves, but that of $|c\rangle$ is 50 times larger ($N_\gamma = 0.1$ and $r_\gamma = 50$). We notice that Poissonian pumping statistics always gives smaller starting times than regular pumping for the same values of the pumping parameter and atomic decay rates. This is because in the Poissonian case, the pumping rate fluctuates around the average. Even though the average might be the same as in the regular case, sometimes the Poissonian pumping rate will be slightly larger than the regular one.

As we have mentioned in the Introduction, trapping states can affect the starting time in a very dramatic way. The most interesting case is when the pumping parameter equals $4\pi N_{\rm ex}$ and all number states become trapping states. For this value of the pumping parameter, the two-photon micromaser never starts, even at finite temperatures. Atomic decay, however, destroys the trapping states, as we saw in Sec. IV. So we expect the micromaser to start when there is some atomic damping. In fact, our model predicts just that, as we can see from Fig. 10, which is a plot of the starting time as a function of the ratio between the decay rates of the lower and the upper energy levels for $N_\gamma = 0.1$, $N_{\rm ex} = 15$, and Poissonian pumping. This was computed numerically at $\varphi_{\rm int} = 4\pi N_{\rm ex}$, where the micromaser with no atomic decay would never start. We notice that the starting time

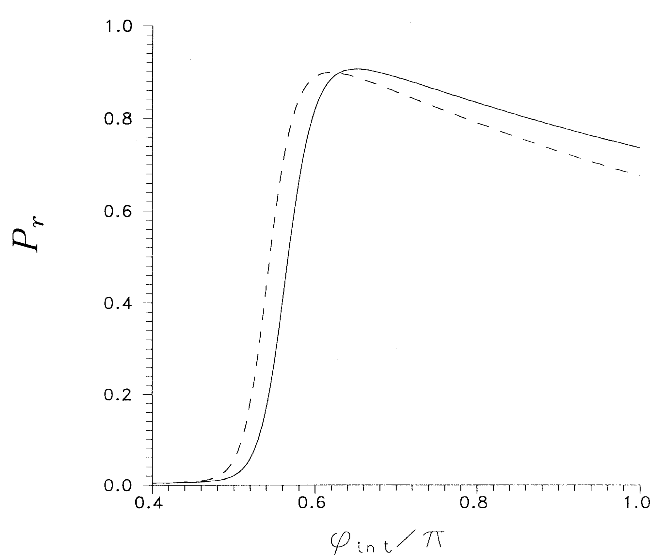

FIG. 8. Probability of detecting an atom exiting the cavity in level $|c\rangle$ as a function of the pumping parameter at the steady state for $N_{\rm ex} = 15$ and regular pumping statistics. The dashed line corresponds to $N_\gamma = 0.1$ and $r_\gamma = 10$. The full line corresponds to $N_\gamma = 0.1$ and $r_\gamma = 50$.

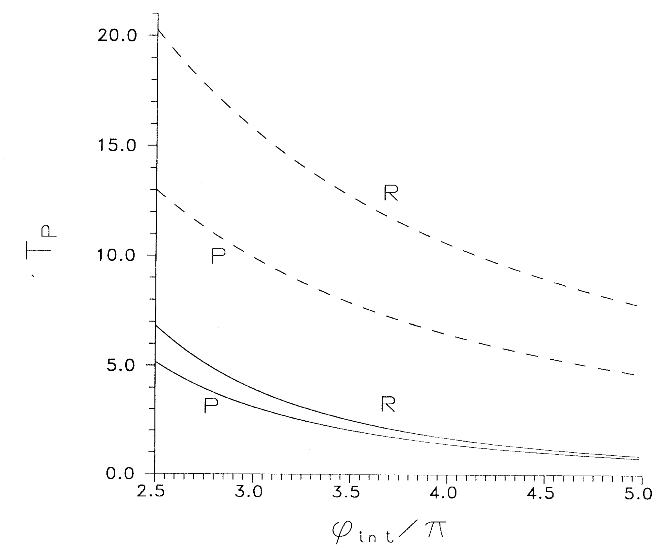

FIG. 9. Starting time as a function of the pumping parameter for both Poissonian (P) and regular (R) pumping statistics. The full curves correspond to $\gamma_a = \gamma_c = 0.2g^2/\Delta$ ($N_\gamma = 0.1$ and $r_\gamma = 1$). The dashed curves correspond to $\gamma_a = 0.2g^2/\Delta$ and $\gamma_c = 50\gamma_a$ ($N_\gamma = 0.1$ and $r_\gamma = 50$). The pumping statistics is indicated by either an R or a P.

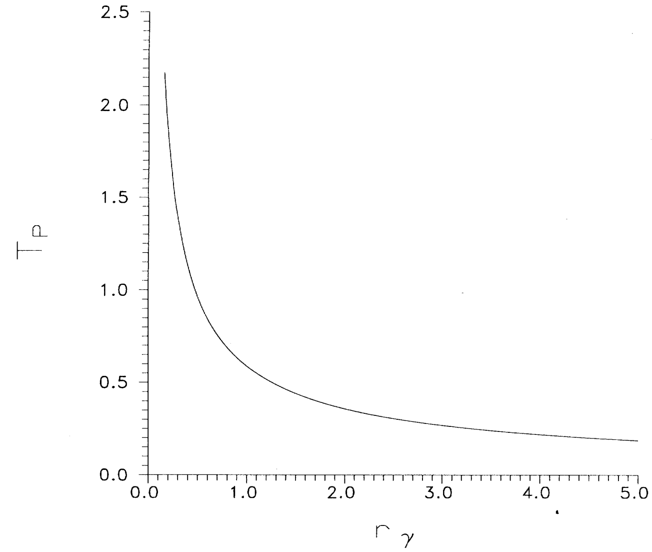

FIG. 10. Starting time as a function of the ratio r_γ. The pumping statistics is Poissonian. $N_{\rm ex} = 15, N_\gamma = 0.1$, and $\varphi_{\rm int} = 4\pi N_{\rm ex}$.

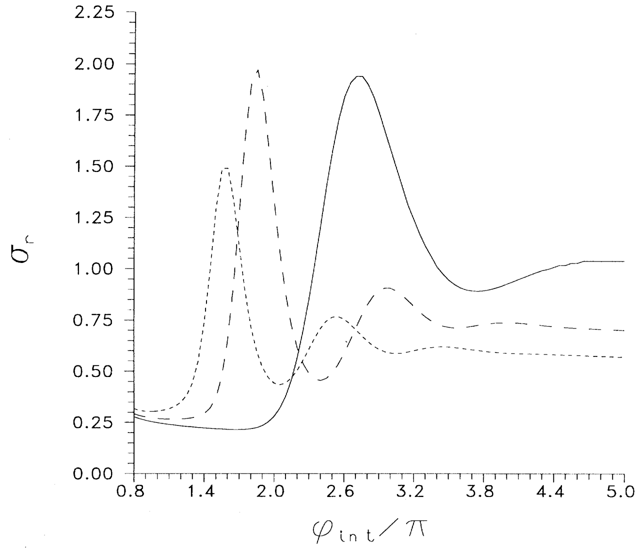

FIG. 11. Photon number variance as a function of the pumping parameter for regular pumping statistics. $N_{\rm ex} = 15$ and $N_\gamma = 0.1$ are fixed. The full line corresponds to $r_\gamma = 1$, the dashed line corresponds to $r_\gamma = 20$, and the dotted line corresponds to $r_\gamma = 50$. We notice that in the micromaser regime the larger the decay rate of $|c\rangle$, the larger the variance. In the laser regime, the opposite occurs. The large peaks are due to the fact that the photon distribution has more than one peak.

decreases as the decay rate of the lower energy level increases. This is because the higher the decay rate of the lower level, the more likely the atom is to decay from the lower level while leaving two photons in the cavity mode. We also notice that when the decay rate of the lower energy level is small the starting time becomes very large. This is because for $\varphi = 4\pi N_{\rm ex}$ and $N_\gamma = 0.1$ we are sufficiently close to the laser regime for reabsorption to hamper the starting process.

VI. NOISE REDUCTION

It is well known that in lasers, inhibition of photon reabsorption leads to noise reduction [23]. This is because atomic decay in lasers makes reabsorption random. Only when the atom does not decay from its lower energy state can it reabsorb photons. Because this decay is random, sometimes an atom will reabsorb photons and sometimes it will not. When the decay rate of the lower energy level is very large, the atom will decay in most cases before it can reabsorb photons and this randomness is suppressed. This leads to smaller fluctuations in the photon number and noise reduction. We have found, however, that the same is not true in the micromaser regime. The reason why this simple argument breaks down in the micromaser regime helps to clarify some of the peculiar physics of micromasers.

Figure 11 shows a plot of the variance in the photon number as a function of the pumping parameter. This was obtained from a numerical calculation using the master equation we have derived for the two-photon micromaser with atomic losses. In these calculations, the pumping statistics is regular. The decay rate of the upper atomic energy level is 0.2 of the effective two-photon coupling constant and $N_{\rm ex} = 15$. There are three curves. One for the case where the decay rate of the lower energy level is the same as that of the upper level (full line), another for the case where it is 20 times larger (dashed line), and the last one for the case where it is 50 times larger (dotted line). We notice that for large $\varphi_{\rm int}$, when we get closer to the laser regime, inhibition of reabsorption does lead to noise reduction. In the micromaser regime, the small pumping parameter region, where we find the smallest variances, we notice, however, that inhibition of reabsorption, far from reducing the noise, actually increases it.

In the micromaser regime, the atomic decay rates are not large enough for the atoms to have a significant probability of decaying while they are still in the cavity. So reabsorption of photons is a dominant effect. It is reabsorption that allows Rabi oscillations to occur. Atom and cavity mode exchange energy quanta back and forth in a coherent and reversible way. This coherent exchange of energy quanta is crucial for the noise reduction mechanism in micromasers. When atomic decay increases, reabsorption starts to become random and the reversible Rabi oscillations start degenerating into an irreversible exchange of energy quanta between the atom and the field mode as in lasers. So reabsorption plays completely different roles in lasers and micromasers. In lasers, reabsorption is an extra undesirable source of noise. In micromasers, it is an essential part of the noise reduction mechanism. Similar results were obtained for the one-photon micromaser in Ref. [24].

Perhaps the most striking feature of Fig. 11 is the presence of a very pronounced peak on each curve just before the laser regime is reached. If we return to Fig. 3 and notice that the photon distribution is related to the effective potential by Eq. (3.3), we see that these peaks correspond to the stage where the photon distribution has developed many peaks and is just about to start smoothing them out on the way to the laser regime where there are two peaks at most.

VII. CONCLUSION

We have shown that atomic decay can affect both the dynamics and the dynamic steady state of two-photon micromasers. Trapping states are easily destroyed by atomic decay even when the average decay time is much longer than the transit time through the cavity. However, in contrast with trapping states in one-photon micromasers, we have found that in two-photon micromasers, trapping states are sensitive to the decay rate of the upper atomic energy level as well as that of the lower. This is a consequence of the Stark shift. We have also shown that reabsorption of photons plays an important part in the starting up mechanism of two-photon micromasers. When reabsorption decreases, the micromaser takes longer to start.

Our model also allows us to go from a micromaser regime, where atomic average decay times are long in comparison with the interaction time, to a laser regime, where atomic average decay times are short. We have found that atomic decay plays very different roles in these two regimes. In the micromaser regime, reabsorption of photons is a fundamental part of both the starting up process and the noise reduction mechanism. So small decay rates for the lower atomic energy level are desirable. In the laser regime, reabsorption of photons is a source of noise and a loss mechanism. So it would seem that large decay rates for the lower atomic energy level are desirable.

ACKNOWLEDGMENTS

This work was supported by the Conselho Nacional de Desenvolvimento Científico e Tecnológico, Coordenação de Aperfeiçoamento de Pessoal de Nível Superior, the European Community, and the United Kingdom Engineering and Physical Sciences Research Council.

[1] S. Haroche and J. M. Raimond, Adv. At. Mol. Phys. **20**, 347 (1985).

[2] D. Meschede, H. Walther, and G. Mueller, Phys. Rev. Lett. **54**, 551 (1985).

[3] M. Brune, J. M. Raimond, P. Goy, L. Davidovich, and S. Haroche, Phys. Rev. Lett. **59**, 1899 (1987).

[4] L. Davidovich, J. M. Raimond, M. Brune, and S. Haroche, Phys. Rev. A **36**, 3771 (1987).

[5] S.-Y. Zhu and L. Z. Wang, Phys. Rev. A **42**, 5798 (1990); S.-Y. Zhu, L. Z. Wang, and H. Fearn, *ibid.* **44**, 737 (1991).

[6] E. S. Guerra, J. Plon, and N. Zagury, Phys. Rev. A **48**, 2261 (1993).

[7] P. Filipowicz, J. Javanainen, and P. Meystre, J. Opt. Soc. Am. B **3**, 906 (1986); P. Meystre, G. Rempe, and H. Walther, Opt. Lett. **13**, 1078 (1988).

[8] C. R. Carvalho, L. Davidovich, and N. Zagury, Opt. Commun. **72**, 306 (1989).

[9] P. Filipowicz, J. Javanainen, and P. Meystre, Phys. Rev. A **34**, 3077 (1986).

[10] E. S. Guerra and N. Zagury, Opt. Commun. **88**, 347 (1992).

[11] E. S. Guerra, A. Z. Khoury, L. Davidovich, and N. Zagury, Phys. Rev. A **44**, 7785 (1991).

[12] V. F. Weisskopf and E. Wigner, Z. Phys. **63**, 54 (1930).

[13] M. Sargent III, M. O. Scully, and W. E. Lamb, Jr., *Laser Physics* (Addison-Wesley, Reading, MA, 1974); W. H. Louisell, *Quantum Statistical Properties of Radiation,* (Wiley, New York, 1973).

[14] M. Brune, J. M. Raimond, and S. Haroche, Phys. Rev. A **35**, 154 (1987).

[15] S. Y. Zhu and X. S. Li, Phys. Rev. A **36**, 3889 (1987).

[16] J. Bergou, L. Davidovich, M. Orszag, C. Benkert, M. Hillery, and M. O. Scully, Opt. Commun. **72**, 82 (1989); Phys. Rev. A **40** , 5053 (1989).

[17] S.-Y. Zhu and X.-S. Li, Phys. Rev. A **36**, 3889 (1987).

[18] E. T. Jaynes and F. W. Cummings, Proc. IEEE **51**, 89 (1963); B. Shore and P. L. Knight, J. Mod. Opt. **40**, 1195 (1993).

[19] S. M. Barnett and P. L. Knight, Phys. Rev. A **33**, 2444 (1986).

[20] T. Quang, P. L. Knight, and V. Buzek, Phys. Rev. A **44**, 6092 (1991).

[21] R. R. Puri and R. K. Bullough, J. Opt. Soc. Am. B **5**, 2021 (1988).

[22] A. M. Guzman, P. Meystre, and E. M. Wright, Phys. Rev. A **40**, 2471 (1989).

[23] F. Haake, S. M. Tan, and D. F. Walls, Phys. Rev. A **40**, 7121 (1989).

[24] L. Z. Wang, S.-Y. Zhu, and J. Bergou, Phys. Rev. A **43**, 2436 (1991).